

## Accepted Manuscript

Discovery of Chiral Dihydropyridopyrimidinones as Potent, Selective and Orally Bioavailable Inhibitors of AKT

Saravanan Parthasarathy, Kenneth Henry, Huaxing Pei, Josh Clayton, Mark Rempala, Deidre Johns, Oscar De Frutos, Pablo Garcia, Carlos Mateos, Sehila Pleite, Yong Wang, Stephanie Stout, Bradley Condon, Sheela Ashok, Zhohai Lu, William Ehlhardt, Tom Raub, Mei Lai, Sandaruwan Geeganage, Timothy P. Burkholder

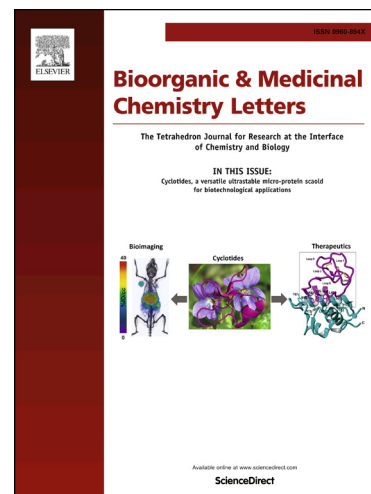
PII: S0960-894X(18)30297-X  
DOI: <https://doi.org/10.1016/j.bmcl.2018.03.092>  
Reference: BMCL 25746

To appear in: *Bioorganic & Medicinal Chemistry Letters*

Received Date: 9 February 2018  
Revised Date: 30 March 2018  
Accepted Date: 31 March 2018

Please cite this article as: Parthasarathy, S., Henry, K., Pei, H., Clayton, J., Rempala, M., Johns, D., De Frutos, O., Garcia, P., Mateos, C., Pleite, S., Wang, Y., Stout, S., Condon, B., Ashok, S., Lu, Z., Ehlhardt, W., Raub, T., Lai, M., Geeganage, S., Burkholder, T.P., Discovery of Chiral Dihydropyridopyrimidinones as Potent, Selective and Orally Bioavailable Inhibitors of AKT, *Bioorganic & Medicinal Chemistry Letters* (2018), doi: <https://doi.org/10.1016/j.bmcl.2018.03.092>

This is a PDF file of an unedited manuscript that has been accepted for publication. As a service to our customers we are providing this early version of the manuscript. The manuscript will undergo copyediting, typesetting, and review of the resulting proof before it is published in its final form. Please note that during the production process errors may be discovered which could affect the content, and all legal disclaimers that apply to the journal pertain.





## Discovery of Chiral Dihydropyridopyrimidinones as Potent, Selective and Orally Bioavailable Inhibitors of AKT

Saravanan Parthasarathy<sup>a,\*</sup>, Kenneth Henry<sup>a</sup>, Huaxing Pei<sup>a</sup>, Josh Clayton<sup>a</sup>, Mark Rempala<sup>a</sup>, Deidre Johns<sup>a</sup>, Oscar De Frutos<sup>b</sup>, Pablo Garcia<sup>b</sup>, Carlos Mateos<sup>b</sup>, Sehila Pleite<sup>b</sup>, Yong Wang<sup>a</sup>, Stephanie Stout<sup>a</sup>, Bradley Condon<sup>c</sup>, Sheela Ashok<sup>c</sup>, Zhohai Lu<sup>a</sup>, William Ehlhardt<sup>a</sup>, Tom Raub<sup>a</sup>, Mei Lai<sup>a</sup>, Sandaruwan Geeganage<sup>a</sup>, and Timothy P. Burkholder<sup>a</sup>

<sup>a</sup>Lilly Research Laboratories, Lilly Corporate Center, Eli Lilly and Company, Indianapolis, IN-46285-0150

<sup>b</sup>Lilly S.A., Avda.de la Industria 30, 28108-Alcobendas, Madrid, Spain

<sup>c</sup>Lilly Research Laboratories, Lilly Biotechnology Center, Eli Lilly and Company, San Diego, CA-92121

### ARTICLE INFO

#### Article history:

Received

Revised

Accepted

Available online

Dedicated to Professor E. J. Corey on the occasion of his 90<sup>th</sup> birthday

#### Keywords:

AKT Inhibitor

GSK3 $\beta$

ATP competitive

Orally Bioavailable

### ABSTRACT

During the course of our research efforts to develop potent and selective AKT inhibitors, we discovered enantiomerically pure substituted dihydropyridopyrimidinones (DHP) as potent inhibitors of protein kinase B/AKT with excellent selectivity against ROCK<sub>2</sub>. A key challenge in this program was the poor physicochemical properties of the initial lead compound **5**. Integration of structure-based drug design and physical properties-based design resulted in replacement of a highly hydrophobic poly fluorinated aryl ring by a simple trifluoromethyl that led to identification of compound **6** with much improved physicochemical properties. Subsequent SAR studies led to the synthesis of new pyran analog **7** with improved cell potency. Further optimization of pharmacokinetics properties by increasing permeability with appropriate fluorinated alkyl led to compound **8** as a potent, selective AKT inhibitors that blocks the phosphorylation of GSK3 $\beta$  in vivo and had robust, dose and concentration dependent efficacy in the U87MG tumor xenograft model

© 2018 Elsevier Ltd. All rights reserved.

AKT, also known as protein kinase B (PKB), is a serine-threonine protein kinase that plays a key role in the phosphatidylinositol-3-kinase (PI3K)/AKT/mammalian target of rapamycin (mTOR) pathway.<sup>1</sup> Increased AKT activation has been implicated in a wide variety of cancers. AKT is identified in three forms with distinct biological relevance: AKT1 is ubiquitously expressed and is the isoform that is believed to play a key role in cancer; AKT2 is highly expressed in muscle, liver and adipocytes and contributes to cell motility and invasion; AKT3 is predominately overexpressed in certain breast, glioma and prostate tumors.<sup>2-4</sup> Based on these factors, many efforts to identify AKT inhibitors with acceptable pharmaceutical properties have been pursued.<sup>5</sup>

However, the discovery of AKT inhibitors having AGC kinase family selectivity has posed a significant challenge due to high homology in the adenosine triphosphate (ATP) binding pocket among the AGC kinase family members. The kinase selectivity over ROCK2 is important since it's another member of the AGC kinase family and is involved in regulation of vascular tone and thus control of blood pressure.<sup>6</sup> There is high homology within the AGC kinase family, with AKT1 and ROCK2 sharing 86%

sequence identity (100% similarity) when the 15 residues within 3 Å of ATP pocket are considered. Several compounds with varying levels of AKT selectivity have been identified, but only a limited number of chemotypes have been reported to have entered early phase clinical trials,<sup>7</sup> including the orally bioavailable dihydropyridopyrimidinone **1** (GDC-0068)<sup>8</sup> and triazolopyrimidine an allosteric AKT inhibitor **2** (MK-2206)<sup>9</sup> (Figure 1).

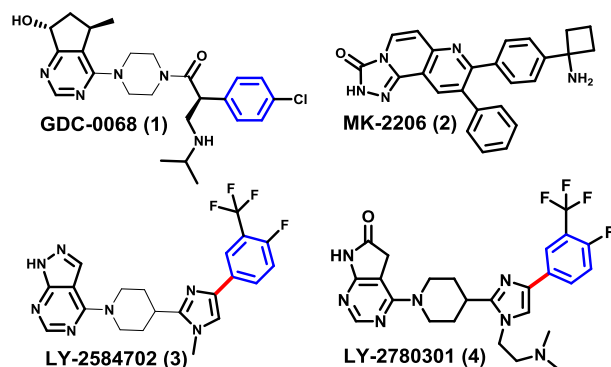
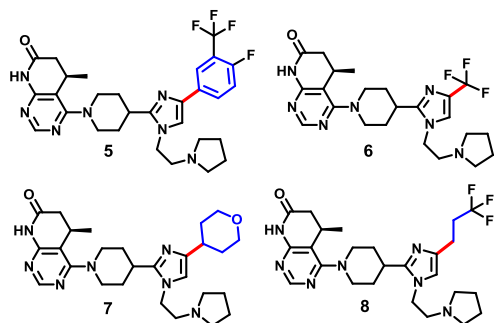


**Figure 1.** ATP competitive type I inhibitor of AKT (**1**), allosteric inhibitor of inactive AKT (**2**), type 1 inhibitor of p70S6K (**3**), and type 1 dual inhibitor of AKT-p70 S6K (**4**)

\* Corresponding author: Tel. +1 317 655 6132. Fax.: +1 317 655 0422  
E-mail address: shakthisarav@gmail.com

We recently described the development of selective p70S6K inhibitor **3** (LY-2584702) and AKT-p70S6K dual inhibitor **4** (LY-2780301) for treatment of advanced solid tumors,<sup>10, 11</sup> we also have pursued development of selective AKT inhibitors for this indication. Here we report for the first time the identification of novel chiral DHP as potent AKT inhibitors with high selectivity for AGC family kinases. Our initial approach was focused on optimizing the hinge binding bicyclic moiety of the inhibitor for selectivity and potency optimization, and then turned our attention to the *N*-alkyl substitution of the imidazole towards optimizing the physicochemical property of our hit series by replacing the aryl-heteroaryl bond with less lipophilic aliphatic substitutions that led to improved aqueous solubility and druglike properties as shown in Figure 2.



Parameter	5	6	7	8
LogP <sup>a</sup>	4.84	1.66	0.95	2.39
Solubility <sup>b</sup> pH7.4	0.035	1.86	>2	0.99
hERG <sup>c</sup>	1.74	>100	>100	18.5

**Figure 2.** Chiral Dihydropyridopyrimidinone AKT Inhibitors (**5-8**), <sup>a</sup>LogP in, <sup>b</sup>Data in mg/mL, <sup>c</sup>Data for hERG dofetilide binding assay in uM.

To guide our attempts at achieving AKT potency and selectivity against p70S6K and other kinases from **3** (p70 S6K IC<sub>50</sub>: 0.004 uM) and **4**, we took advantage of exploiting the subtle sequence differences in the active sites of the AGC family kinases, we utilized the information around crystal structure of AKT1 at the hinge region with analogs of **3-4**.

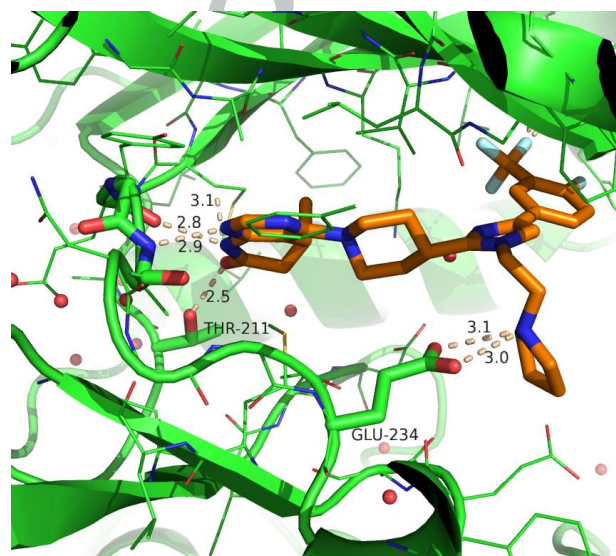


**Figure 3.** X-ray crystal structure of **5** bound to AKT1. Resolution = 2.2 Å, PDB code 6CCY.

During this Hit optimization, through several scaffold morphing steps we have discovered chiral DHP **5** as potent and selective AKT inhibitor. A crystal structure of **5** in complex with AKT1 confirmed the presence of key hydrogen bonds from the amine group of the ligand and to Glu-234 of the protein back bone that is necessary for the AKT1 biological activity. Among the hydrogen bond donors we explored in this region *N*-ethyl pyrrolidine provided the best potency and improved metabolic stability profile. In addition, the dramatic improvement of cell potency with *R* enantiomer of the lactam could be rationalized by chiral methyl group nicely accommodating the lipophilic pocket near the hinge binder region, whereas the *S* enantiomer had sterically hindered effect with protein backbone with loss biological activity. To characterize the kinase selectivity of **5** and its analogs, we profiled their ability to inhibit a panel of ~100 in vitro expressed human protein kinases assays and many of them with IC<sub>50</sub> values listed in Table 1.

**Table 1.** In vitro characterization and Kinase Selectivity<sup>a</sup>

Parameter	5	6	7	8
AKT1	0.003	0.011	0.004	0.005
P70S6K	0.035	0.876	1.90	0.399
ROCK2	>20	>20	>20	>20
PKA	0.653	0.124	0.412	0.084
PKCβ2	0.036	16.3	20	3.98
RSK1	0.020	0.272	0.699	0.568
pGSK3β	0.039	2.46	0.230	0.092

<sup>a</sup>The remaining kinases (>90) have IC<sub>50</sub> values of >20 uM. Where <sup>b</sup>Measured at the apparent ATP *K<sub>m</sub>*, <sup>c</sup>Each value represents the average of ≥2 independent experiments, where each experiments considered of a single determination.

In general, the DHP war head demonstrated high AKT selectivity in enzyme and low activity against ROCK2 and many other kinases (90 Kinases had <80% inhibition at 1 uM, >1000-fold selectivity over ROCK2). The key difference between AKT1 and ROCK2 in the ATP binding site is the gate keeper pocket where there is a favorable hydrogen bond interaction from the carbonyl moiety of the hinge binder with Thr-211 hydroxyl group of AKT1, however in ROCK2 the gatekeeper residue is Val-153. A summary of this structure based drug design, which led to the discovery of potent and selective carbonyl containing chiral dihydropyridopyrimidinone hinge binder **5** as AKT inhibitors, is shown in Figure 3.<sup>12</sup> While **5** and related analogs had attractive cell potency, a major challenge in optimization of this series was a struggle with poor physicochemical properties. Lipophilic compound **5** (LogP/D = 4.84) suffered from relatively high plasma protein binding, poor aqueous solubility (0.035 mg/mL at pH = 7.4) and hERG activity.<sup>13</sup> While the addition of lipophilicity improved potency, clearance and solubility further deteriorated. Alternately, if polar functional groups were simply appended to the periphery of the hinge binder, then potency was compromised and passive permeability decreased.

Thus, the focus of further work was to determine whether analogues could be generated with better solubility and permeability while maintaining the kinase selectivity. With this goal in mind, our medicinal chemistry strategy was therefore to investigate the lipophilic P-loop pocket of lead compound **5** where the fluorinated aryl ring occupies. We reasoned that if we could reduce the molecular weight and co-planarity of **5** on the aryl- heteroaryl junction, then we might improve physicochemical characteristics and in vivo ADME properties.<sup>14</sup>

With the aim of deconstructing the aryl ring, we made the rational design decision of introducing smaller hydrophobic trifluoromethyl substitutions at the imidazole represented by compound **6**. Replacement of the aryl ring with an aliphatic substitutions lowered logP by >2 units and led to increased aqueous solubility, lack of hERG binding and decreased unbound intrinsic clearance (Fig 2).

Although compound **6** and analogues was sufficiently potent in enzyme with >10 fold selectivity for many of the AGC kinase family member, cell potency remained less attractive. We hypothesized that reducing the ring size followed by significant changes to planarity at the P-loop pocket resulted in a dramatic loss of cell activity. On the basis of structural guidance, our attention was directed towards identifying a similarly sized saturated aliphatic ring at the P-loop pocket that might mimic the aryl ring and spatially suitable enough for accommodating the hydrophobic pocket.<sup>15</sup> With this goal in mind we rationalized that symmetrical 4-pyran could be an appropriate saturated ring that could fit well without significantly increased hydrophobicity. Replacing the trifluoromethyl substitution with six-membered 4-pyran as compound **7** that resulted in 10 fold boost in both cell and enzyme potency.

Gratifyingly, compound **7** also demonstrated improved physicochemical properties with significant improvement in aqueous solubility. Compound **7** was sufficiently potent to determine its pharmacokinetic (PK) and pharmacodynamics (PD); data is summarized in Table 2.

**Table 2.** ADME Properties of Lead **6-8**<sup>a</sup>

Parameter	<b>6</b>	<b>7</b>	<b>8</b>	Units
Dose (IV/PO)	10, 5	10, 5	10, 5	mg/kg
Bioavailability	64	14	55	%
AUC <sub>0-24h, PO</sub>	24100	173	638	ng.h/mL
CL	2.18	64	74	mL/min/kg
Intrinsic CL <sub>u</sub> <sup>b</sup>	66	85	43	mL/min/kg
V <sub>dss</sub>	0.65	13.8	11.6	L/kg
T <sub>1/2</sub>	3	8.6	2.3	h
MDCK P <sub>pass</sub> <sup>c</sup>	410	60	200	nm/sec
P-gp Efflux Ratio	29	82	54	

<sup>a</sup>Measured data for compound fraction unbound to human plasma protein, AUC<sub>0-24</sub> Area under the plasma concentration time curve from 0-24 hours post-dosing, All data generated in SD rats, Values are an average of n= 3 animals, Data reported using a 5 mg/kg PO dose and 10 mg/kg IV dose. <sup>b</sup>Scaled intrinsic unbound clearance in mL/min/Kg. <sup>c</sup>Passive permeability coefficient (P<sub>pass</sub>) was measure bidirectionally in duplicate across confluent monolayers of MDCK-MDR1 cells with inhibition of P-gp.

Table 2 shows ADME characteristics for compound **6** and **7** as a result of reduced hydrophobicity. Indeed, while the introduction of 4-pyran in the place of CF<sub>3</sub>- enhances the cell potency, and maintained its selectivity. A key issue at this stage was poor oral exposure, low bioavailability and reduced passive permeability with increased plasma clearance.<sup>16</sup> This presented us with conundrum in that although the pyran ring was the most efficient replacement for the aryl ring in terms of hydrophobicity/potency (LogP = 0.95), it suffered from poor permeability and low oral exposure. Compound **6** had been shown to be a substrate for P-glycoprotein (P-gp) in vitro (Table 2), but this did not appear to impact its oral absorption. With the decrease in P<sub>pass</sub> of compound **7** and increase in efflux ratio, we suspected that oral

absorption of compound **7** might be impacted by P-gp mediated efflux.

Therefore, to confirm oral absorption impacted by increased P-gp efflux, we examined oral exposure of compound **7** in P-gp and breast cancer resistance protein (Bcrp) KO mice.<sup>17</sup> Compound **7** had 5 fold greater plasma exposure in P-gp KO mice compared to normal mice at the same dose (Table 3). Bcrp alone and together with P-gp was not a factor, which was consistent with in vitro results showing that compound **7** is not a Bcrp substrate.

**Table 3.** P-gp Properties of Lead **7-8**<sup>a</sup>

Parameter	<b>7</b>	<b>8</b>	Units
AUC <sub>0-24h, PO, wt</sub>	108	290	ng.h/mL
AUC <sub>0-24h, PO, TKO</sub>	501	359	ng.h/mL
C <sub>max, wt</sub>	33	76	ng/mL
C <sub>max, TKO</sub>	189	109	ng/mL
TPSA <sup>b</sup>	88	79	
HBA Strength <sup>c</sup>	13.9	12.2	

<sup>a</sup>AUC<sub>0-24</sub> Area under the plasma concentration time curve from 0-24 hours post-dosing, All data generated in normal or wild-type and P-gp/Bcrp knockout or mdr1a,b(-/-, -/-) and abcg2 (-/-) triple genotype mice, Values are an average of n= x animals, Data reported using a 2.5 mg/kg PO dose. <sup>b</sup>Predicted Topological polar surface area. <sup>c</sup>Total strength of hydrogen bond acceptors predicted using.

Both passive permeability and P-gp substrate recognition appeared to change with relative constancy of hydrogen bond (HB) count and topological polar surface area (TPSA). So, based upon a negative relationship between P<sub>pass</sub> and total HB strength and a positive relationship between P-gp efflux ratio and total HB strength (Table 2 and 3). We focused on reducing total HB strength especially with regard to imidazole substitutions. So, we decided to revisit the fluorinated alkyl substituent that could maintain the potency with improved permeability.<sup>18</sup> We reasoned that if we could extend the alkyl chain farther (from simple -CF<sub>3</sub> substitution **6**) while reaching into the enzyme p-loop pocket deep enough, then that should maintain its activity similar to the aryl (**5**) or cyclic ring (**7**) system.<sup>15</sup> In addition, such a fluorinated alkyl group with reduced polarity and hydrogen bond accepting strength should improve passive permeability and decrease the P-gp effect. To validate our design hypothesis, we synthesized trifluoropropyl substituted compound **8** as shown in scheme 3.

In vivo PK parameters obtained in rat after intravenous administration at 10 mg/kg and oral dosing at 5 mg/kg are highlighted in Table 2. Replacing the fluorinated aryl ring **5** and hydrophilic 4-pyran in **7** with an appropriate fluorinated alkyl led to compound **8** displaying improved permeability and oral bioavailability in rat as expected. PK attributes were also favorable in mouse and dog (data not shown in manuscript preparation). In addition, compound **8** demonstrated enhanced cell potency and ideal physicochemical properties. Based on these encouraging results compound **8** was tested in vivo for efficacy in a 4 weeks U87MG rat xenograft model. Oral doses were chosen to be 25, 50 mg/kg once or 25 mg/kg twice, daily as crystalline suspensions in Hydroxyethyl cellulose (HEC). Tumor volume was measured relative to controls animal treated with HEC vehicle only. Compound **8** induced dose-dependent growth inhibition and was well tolerated with no body-weight loss observed at all doses and dose regimens tested.

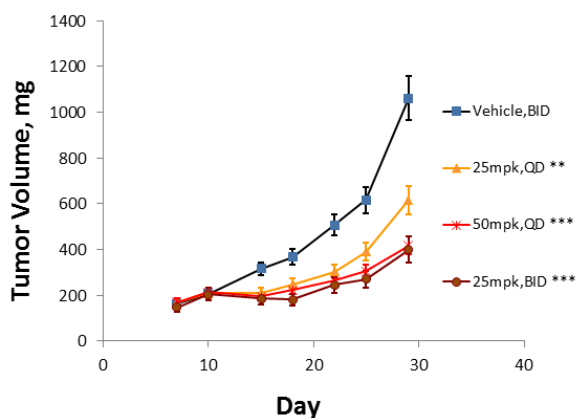
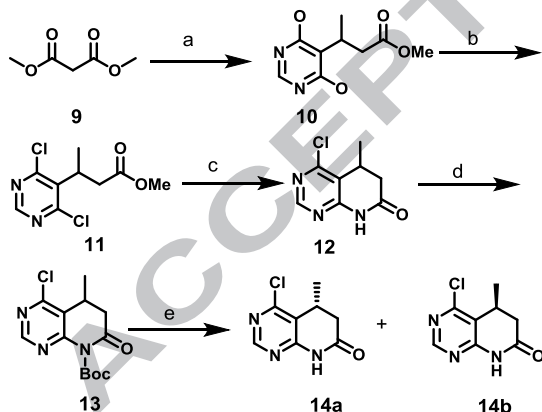


**Figure 5.** In vivo efficacy of compound **8** in a 28 day mouse U87MG xenograft model

The synthesis of final compounds **5-8** is outlined in Scheme 1-3. The synthesis of enantiomerically pure (*R*)- and (*S*)-4-chloro-5-*R*<sup>1</sup>-6,8-dihydro-5H-pyrido[2,3-*d*]pyrimidin-7-one started from commercially available propanedioic acid dimethyl ester **9** subjected for Michael addition with methyl crotonate ((*E*)-methyl but-2-enoate) followed by an in situ ring formation to give **10**. Compound **10** was prepared by chlorination of the hydroxyl group with POCl<sub>3</sub> in the presence of base such as *N,N*-diethylaniline. The racemic compound **12** was obtained by treating excess amount of aqueous ammonium hydroxide. In order to improve the throughput of the chiral resolution **12** was further protected as *N*-Boc derivative by treating with Boc anhydride in the presence of DMAP to provide **13**. The chiral lactam **14a** was prepared by chiral chromatography and subsequent removal of the protecting group under acidic condition furnished the final compound with good optical purity.

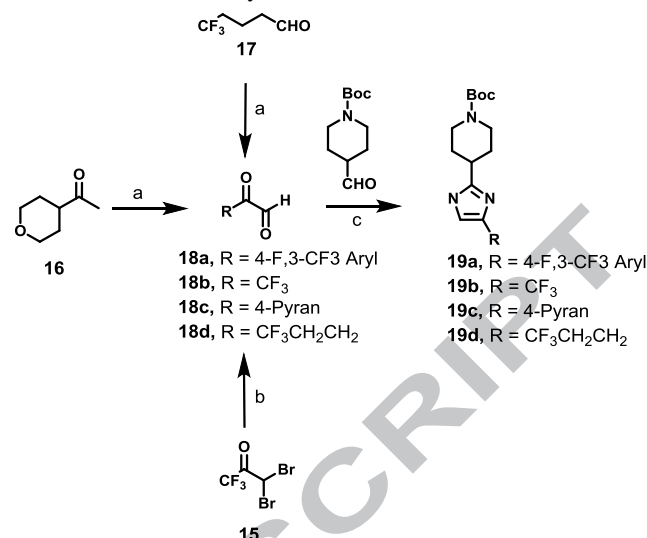
### Scheme 1. War Head Synthesis<sup>a</sup>



<sup>a</sup> Reagents and Conditions: (a) (i) NaOMe, ethyl crotonate, MeOH, 70 °C, (ii) Formamidinium acetate, -20 °C-RT; (b) POCl<sub>3</sub>, MeCN, Et<sub>2</sub>NPh, 85 °C; (c) NH<sub>3</sub> in iPrOH, 65 °C; (d) (Boc)<sub>2</sub>O, DMAP, CH<sub>2</sub>Cl<sub>2</sub>, room temp.; (e) chiral HPLC chromatography, 4M HCl in Dioxane, room temp.

Scheme 2 shows the synthesis of imidazole intermediates **19a**, **19b**, **19c** and **19d**. The key precursor keto aldehyde **18a-18d** was prepared in situ by SeO<sub>2</sub> mediated oxidation of corresponding carbonyl compounds **16** and **17** or hydrolysis of dibromo ketone **15**. Subsequent treatment with *N*-Boc piperidine-4-carbaldehyde in the presence of aqueous NH<sub>4</sub>OH afforded the respective imidazoles in good yield.

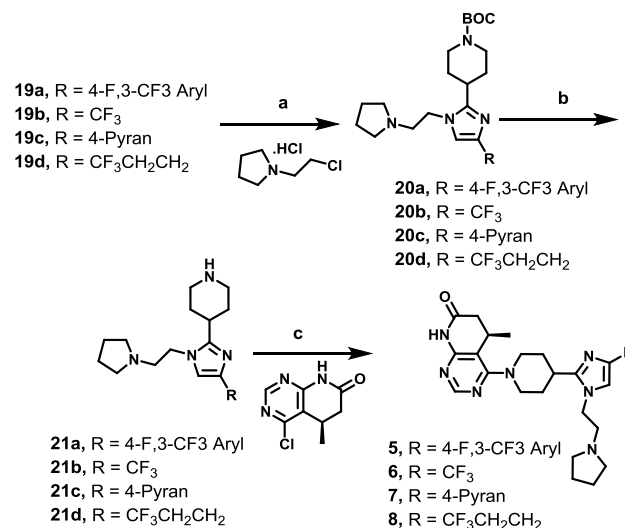
### Scheme 2. Imidazole Synthesis<sup>a</sup>



<sup>a</sup> Reagents and Conditions: (a) (i) SeO<sub>2</sub>, AcOH, Dioxane-H<sub>2</sub>O, 90 °C, (b) NaOAc, H<sub>2</sub>O, 90 °C; (c) Aq. NH<sub>4</sub>OH, MeOH, 30 °C.

Shown in Scheme 3, is a convergent synthetic route to final compounds **5-8**. The key intermediates **21a-21d** were made by reacting imidazole **19a-19c** and **19d** with 1-chloro ethyl pyrrolidine HCl salt in the presence of base resulted in alkylated imidazole derivatives **20a-20d**, followed by trifluoroacetic acid mediated deprotection gave the corresponding piperidines. With the requisite piperidine amine and chiral Core **14a** in hand, preparation of the desired compounds was accomplished by base promoted S<sub>N</sub>Ar reaction to give **5-8**.

### Scheme 3. Convergent Synthesis<sup>a</sup>



<sup>a</sup> Reagents and Conditions: (a) (i) KOH, DMSO, 25 °C; (b) Aq.HCl, iPrOH, 50 °C; (c) Et<sub>3</sub>N, *N*-methylpyrrolidinone, 110 °C.

In summary, we have outlined the optimization of **5** to advanced molecules such as **8** using a combination of both structure- and physical-property-based design parameters.<sup>19</sup> We have identified chiral dihydropyridopyrimidinone as a unique kinase inhibitor scaffold of AKT with ROCK2 selectivity, the pharmacological activity resides almost exclusively in the (*R*)-enantiomer. In addition, the cyclic amine pyrrolidine provided optimum AKT potency and metabolic stability. Furthermore, the aliphatic substituent in place of the aryl ring of the imidazole lead **6** served

non planar system and to provide a platform for optimizing the physical properties of the resulting molecules. During lead optimization, changes in LogP highlighted valuable structural modifications and restrained the overuse of lipophilicity, which ultimately provided more balanced molecules. As a result, **8** was investigated elaborately for preclinical development and represents a broadly selective, potent, ATP-competitive AKT inhibitor.

### Supplementary data

Supplementary data (Experimentals for the synthesis of compound **7** and procedures for AKT1 and ROCK2 binding and GSK3 $\beta$  cell assays.) associated with this article can be found, in the online version, at <http://>.

### Acknowledgement

We thank Gerri Sawada, Karen Huss and Laura Bloem for their help in *in vitro* evaluations of compound. We acknowledge the cloning work for the crystallography construct done by Aiping Zhang and the scientific leadership by Devon Thompson in the early crystallography enablement. This research used resources of the Advanced Photon Source, a U.S. Department of Energy (DOE) Office of Science User Facility operated for the DOE Office of Science by Argonne National Laboratory under Contract No. DE-AC02-06CH11357. Use of the Lilly Research Laboratories Collaborative Access Team (LRL-CAT) beamline at Sector 31 of the Advanced Photon Source was provided by Eli Lilly Company, which operates the facility.

### References and notes

- Manning, B.; Cantley, L. C. AKT/PKB Signaling Navigating Downstream. *Cell* **2007**, *129*, 1261–74.
- Hers, I.; Vincent, E. E.; Tavaré, J. M. Akt signalling in health and disease. *Cellular Signaling* **2011**, *23*, 1515–27.
- Pereira, L.; Horta, S.; Mateus, R.; Videira, M. A. Implications of Akt2/Twist crosstalk on breast cancer metastatic outcome. *Drug Disc. Today* **2015**, *20*, 1152–58.
- Turner, K. M.; Sun, Y.; Ji, P.; Granberg, K. J.; Bernard, B.; Hu, L.; Cogdell, D. E.; Zhou, X.; Yli-Harja, O.; Nykter, M.; Shmulevich, I.; Yung, A.; Fuller, G. N.; Zhang, W. Genomically amplified Akt3 activates DNA repair pathway and promotes glioma progression. *Proc. Natl. Acad. Sci.* **2015**, *112*, 3421–26.
- Mattmann, M. E.; Stoops, S. L.; Lindsey, C. W. Inhibition of Akt with small molecules and biologics: Historical perspective and current status of the patent landscape. *Expert Opin. Pat.* **2011**, *21*, 1309–38.
- Takahara, A.; Sugiyama, A.; Yoneyama, M.; Hashimoto, K. Cardiovascular effects of Y-27632, a selective Rho-associated kinase inhibitor, assessed in the halothane-anesthetized canine model. *Eur. J. Pharmacol.* **2003**, *460*, 51–57.
- Martini, M.; De Santis, M. C.; Braccini, L.; Gulluni, F.; Hirsch, E. PI3K/AKT signaling pathway and cancer: an update review. *Annals of Medicine* **2014**, *46*, 372–383.
- Blake, J. F.; Xu, R.; Bencsik, J. R.; Xiao, D.; Kallan, N. C.; Schlachter, S.; Mitchell, I. S.; Spencer, K. L.; Banka, A. L.; Wallace, E. M.; Gloor, S. L.; Martinson, M.; Woessner, R. D.; Vigers, G. P.; Brandhuber, B. J.; Liang, J.; Safina, B. S.; Li, J.; Zhang, B.; Chabot, C.; Do, S.; Lee, L.; Oeh, J.; Sampath, D.; Lee, B. B.; Lin, K.; Leiderer, B. M.; Skelton, N. J. Discovery and preclinical pharmacology of a selective ATP competitive Akt inhibitor (GDC-0068) for the treatment of human tumors. *J. Med. Chem.* **2012**, *55*, 8110–27.
- Hirai, H.; Sootome, H.; Nakatsuru, Y.; Miyama, K.; Taguchi, S.; Tsuijioka, K.; Ueno, Y.; Hatch, H.; Majumder, P. K.; Pan, B.-S.; Kotani, H. MK-2206, an allosteric Akt inhibitor, enhances antitumor efficacy by standard chemotherapeutic agents or molecular targeted drugs *in vitro* and *in vivo*. *Mol. Cancer Ther.* **2010**, *9* (7), 1956–67.
- Tolcher, A.; Goldman, J.; Patnaik, A.; Papadopoulos, K. P.; Westwood, P.; Kelly, C. S.; Bumgardner, W.; Sams, L.; Geeganage, S.; Wang, T.; Capen, A. R.; Huang, J.; Joseph, S.; Miller, J.; Benhadji, K. A.; Brail, L. H.; Rosen, L. S. A phase I trial of LY 2584702 tosylate, a p70 S6 kinase inhibitor, in patients with advanced solid tumors. *Eur. J. Cancer* **2014**, *50*, 867–75.
- Azaro, A.; Rondon, J.; Calles, A.; Brana, I.; Hidalgo, M.; Lopez-Casas, P. P.; Munoz, M.; Westwood, P.; Miller, J.; Moser, B. A.; Ohnmacht, U.; Bumgardner, W.; Benhadji, K. A. A first-in-human phase I trial of LY 2780301, a dual p70 S6 kinase and Akt inhibitor, in patients with advanced or metastatic cancer. *Invest. New Drugs* **2015**, *33*, 710–19.
- Parthasarathy, S.; Burkholder, T. P.; Pei, H.; Clayton, J. R.; Rempala, M.; Henry, K. J.; Eggen, M. J.; Johns, D. M.; Sawyer, S.; Beight, D. J.; Preparation of chiral dihydropyridopyrimidinone as inhibitors of AKT. WO2011050016.
- Shamovsky, I.; Connolly, S.; David, L.; Ivanova, S.; Norden, B.; Springthorpe, B.; Urbahna, K. Overcoming Undesirable hERG Potency of Chemokine Receptor Antagonist Using Baseline Lipophilicity Relationship. *J. Med. Chem.* **2008**, *51*, 1162–78.
- Ishikawa, M.; Hashimoto, Y. Improvement in Aqueous Solubility in Small Molecule Drug Discovery Programs by Disruption of Molecular Planarity and Symmetry. *J. Med. Chem.* **2011**, *54*, 1539–54.
- Patel, R. Y.; Doersken, R. J. Protein Kinase-Inhibitor Database: Structural Variability and Inhibitor Interactions with the Protein Kinase P-Loop. *J. Prot. Res.* **2010**, *9*, 4433–42.
- Varma, M. V. S.; Obach, R. S.; Rotter, C.; Miller, H. R.; Chang, G.; Steyn, S. J.; El-Kattan, A.; Troutman, D. Physicochemical Space for Optimum Oral Bioavailability: Contribution of Human Intestinal Absorption and First-Pass Elimination. *J. Med. Chem.* **2010**, *53*, 1098–08.
- Hitchcock, S. A. Structure Modifications that Alter the P-Glycoprotein Efflux Properties of Compounds. *J. Med. Chem.* **2012**, *55*, 4877–95.
- Hagmann, W. K. The Many Roles for Fluorine in Medicinal Chemistry. *J. Med. Chem.* **2008**, *51*, 4359–69.
- See supplementary material for crystallography details of **5**.

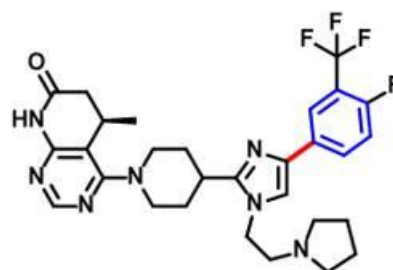
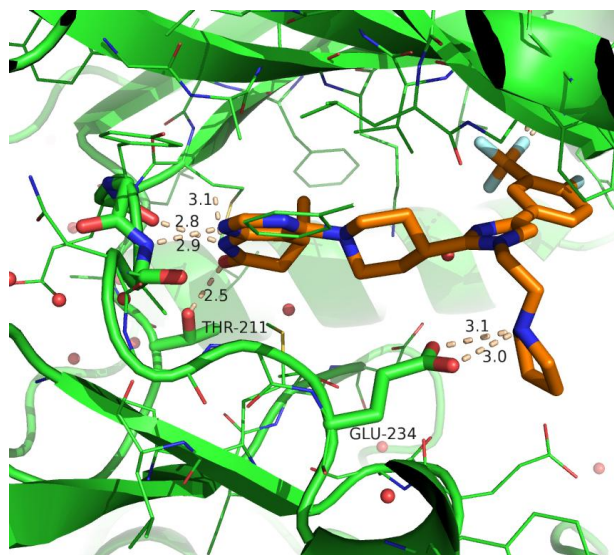
**Graphical Abstract**

To create your abstract, type over the instructions in the template box below.

## Discovery of Chiral Dihydropyridopyrimidinones as Potent, Selective and Orally Bioavailable Inhibitors of AKT

Leave this area blank for abstract info.

Saravanan Parthasarathy<sup>a,\*</sup>, Kenneth Henry<sup>a</sup>, Huaxing Pei<sup>a</sup>, Josh Clayton<sup>a</sup>, Mark Rempala<sup>a</sup>, Deidre Johns<sup>a</sup>, Oscar De Frutos<sup>b</sup>, Pablo Garcia<sup>b</sup>, Carlos Mateos<sup>b</sup>, Sehila Pleite<sup>b</sup>, Yong Wang<sup>a</sup>, Stephanie Stout<sup>a</sup>, Bradley Condon<sup>c</sup>, Sheela Ashok<sup>c</sup>, Zhohai Lu<sup>a</sup>, William Ehlhardt<sup>a</sup>, Tom Raub<sup>a</sup>, Mei Lai<sup>a</sup>, Sandaruwan Geeganage<sup>a</sup>, and Timothy P. Burkholder<sup>a</sup>



AKT1 IC<sub>50</sub>: 0.003  $\mu$ M  
pGSK3 $\beta$  IC<sub>50</sub>: 0.039  $\mu$ M

Fonts or abstract dimensions should not be changed or altered.

**Highlights of the Paper:**

- Chiral DHP as hinge binder provided high AKT1 selectivity over ROCK2/AGC kinases
- Emphasis on physicochemical properties over potency led to developable compounds
- Reducing the HB acceptor strength of compounds with high P-gp efflux improved P<sub>pass</sub>

ACCEPTED MANUSCRIPT